JOURNAL OF MATERIALS SCIENCE 5 (1970) 1005–1010

Magnetic Hysteresis Properties of Internally Oxidised Ni-Si Alloys

R. BARLOW, P. J. GRUNDY
Department of Pure and Applied Physics, University of Salford, Salford 5, UK

Results are presented of magnetic hysteresis measurement made on some internally oxidised Ni-Si alloys. The alloys investigated were originally of nominal composition 0.058, 0.48, 0.77 and 0.96 wt % Si in Ni. Hysteresis loops have been obtained for all the alloys in both unoxidised and several internally oxidised states using a standard technique. The effect of the internal oxide precipitation on the coercivity and remanence of the specimens is made clear by these measurements. The dependence of coercivity on precipitate morphology and alloy compositions is considered and results of the variation of coercivity with the temperature of measurement in the range 20 to 265° C are discussed.

1. Introduction

The kinetics of internal oxidation and details of the precipitate morphology in some internally oxidised Ni-Si alloys have been reported previously [1, 2]. It was suggested in [2] that such systems might have application in testing theories of magnetic coercivity due to non-magnetic inclusions and as mechanically stabilised dispersion-strengthened magnetic material for high temperature service [3, 4].

The results of [2] showed that the precipitate morphology varied from discrete, spheroidal silica particles to extended growths of silica at differing temperatures of oxidation and also through the thickness of a sample (i.e. in a direction normal to the oxidation front). Because of this, the results presented here cannot be applied rigorously to any particular theory of coercivity, except perhaps to a simple relation concerning the volume fraction of second phase, but nevertheless the predominant contributions to coercivity and remanence can be pointed out.

Of relevance to the use of these systems as dispersion-strengthened magnetic material is the dependence of coercivity on temperature. Soft magnetic properties are required and although dispersion-strengthened nickel would not be an ideal choice, because of its low saturation magnetisation and Curie point, measurements on these systems point to the expected dependence in cobalt and cobalt-iron alloys. From recent work it seems that internally oxidised cobalt alloys fit our requirements more closely and it is hoped to report their structural and magnetic properties at a later date.

2. Specimen Preparation and Experiment

Specimens of the alloys were prepared in a suitable form for hysteresis loop measurement by spark-machining flat toroids from 200 μm thick rolled polycrystalline sheet. Any damage or strain introduced by this treatment was removed by vacuum-annealing the specimens at 600° C for 24 h. Internal oxidation was carried out, as previously described [2, 3], at various temperatures and for times sufficient to ensure complete internal oxidation. The calculated times for oxidation through the thickness of the specimens were obtained from the results of [2] and [4].

Specimens for loop measurements consisted of two oxidised toroids separated by a polyethylene washer and sandwiched between two paxallin washers. This protection was intended to avoid the introduction of strains into the toroids when primary (magnetising) coils and secondary (flux) coils were wound onto the assembly. "Air"-flux induced into the non-ferromagnetic parts of the assembly on magnetisation was cancelled by a compensating assembly connected in opposition. Hysteresis loops were plotted continuously on a Hewlett-Packard X-Y chart recorder connected to the output of an Elektro-Physik EF2A fluxmeter and a standard resistance in the magnetising circuit. The toroids were magnetised between field limits of $\pm$ 130 Oe, fig. 1 is an example of a loop obtained on a Ni-0.77 wt % Si alloy.

Remanence was obtained as a fraction of the saturation induction and coercivity was read from the chart calibrated using a formula for the true magnetising field [5].

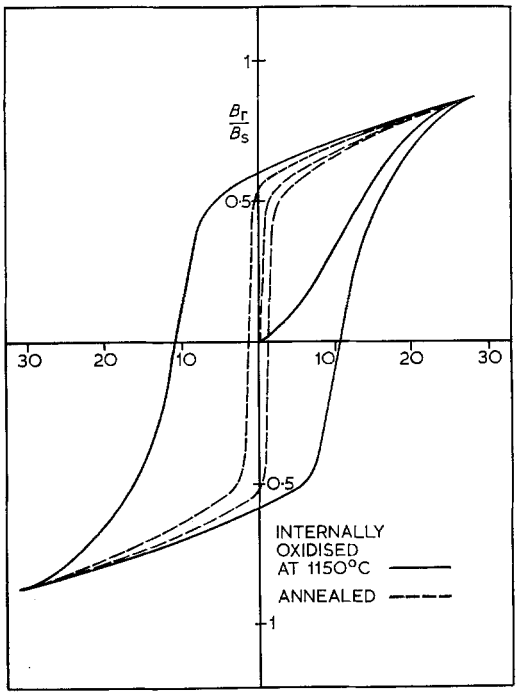

Figure 1 Hysteresis loops for a Ni-0.77 wt % Si alloy specimen measured at room temperature before and after internal oxidation.

For each alloy system under consideration a specimen assembly containing annealed unoxidised material was prepared. These specimens acted as reference samples and allowed the increase in coercivity due to the internal oxidation procedure to be determined. To test the effect of heat-treatment at the high temperatures used in the internal oxidation on the magnetic properties of the alloys through possible changes in the structural state, i.e. grain size, internal strains, defects, etc, toroids of spectroscopically pure nickel were prepared. The hysteresis loop was plotted after vacuum-annealing at 600° C for 24 h and again after a mock "internal oxidation" treatment at 1050° C for 3 h. The remanent flux density and coercive force remained virtually unchanged and it was therefore assumed that any changes in the loop parameters after internal oxidation of the alloys was due solely to the presence of non-magnetic inclusions and any matrix strains or defects associated with them.

The effect of the temperature of measurement on the coercivity of the alloys was investigated by suspending the specimen and compensating assemblies in a simple high-temperature oil bath.

3. Results and Discussion

The remanent induction values measured for the four alloys in both the annealed and internally oxidised states are shown in fig. 2, in relation to the temperature of oxidation. In the two more dilute alloys the remanence is virtually unaffected by the presence of the silica inclusions, being approximately the same as the annealed value and equal to about half the saturation induction.

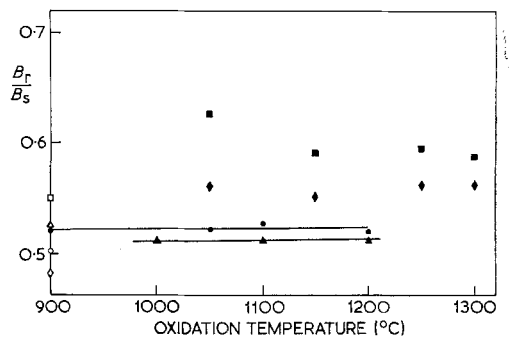

Figure 2 Room temperature measurements of fractional remanence of the internally oxidised alloys as a function of the oxidising temperature. Open symbols are values in the annealed state before internal oxidation. ●–0.058 wt% Si; ▲–0.48 wt % Si; ■–0.77 wt % Si and ♦–0.96 wt % Si.

This result suggests that magnetisation rotation is unhindered and domains of reverse magnetisation are created primarily at the toroid surfaces and grain boundaries. In the two more concentrated alloys there is a slight increase in remanence after oxidation. In these alloys, part at least of the matrix is split up into isolated regions by large-scale silica growths [2] (see figs. 3a and b), thus restricting the growth of reverse domains and resulting in a larger remanence. Within the accuracy of measurement the remanent induction is not sensitive to the temperature of oxidation.

As expected, hysteresis plots for the oxidised specimens revealed an increase in coercivity from those in the annealed state and an increasing coercive force with volume fraction of precipitate. It was also found that the coercivity was dependent to some extent upon the oxidising

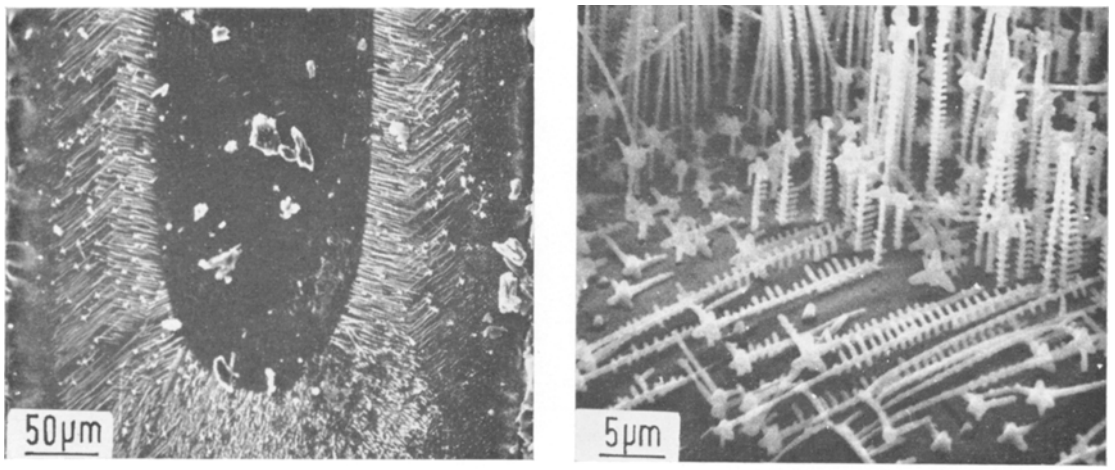

(a) (b)

Figure 3 Scanning electron micrograpns of sections of a Ni-0.77 wt % Si alloy internally oxidised at 1150° C showing (a) the oxidation front after incomplete oxidation and the change of precipitate morphology with depth (× 180); (b) side-branched filamentary growths of silica (× 1600).

temperature used, as shown in fig. 4, especially for the more concentrated alloys. Maximum values of coercivity shown by the 0.48, 0.77 and 0.96 wt % Si alloys are probably associated with the precipitate morphology, as will be discussed later. In the most dilute alloy the coercivity was observed to increase slightly with the oxidising temperature in the range investigated.

3.1. Coercivity and Volume Fraction of Silica

The dependence of the coercivity increase, ΔH_c, over the annealed value on the volume fraction of internal oxide α is shown in fig. 5. The error marks for the four alloys cover the spread of values of ΔH_c for oxidation at the different temperatures used. It is clear that the increase in coercivity is proportional to the volume fraction of oxide present. An expression which can be applied to the systems under investigation is that put forward by Néel [6a]

$$\Delta H_c(1) \simeq \frac{2\alpha K}{\pi I_m}\left\{0.4 + \tfrac{1}{2}\ln\frac{2\pi I_m^2}{K}\right\} \qquad (1)$$

for the increase in coercivity due to domain wall inclusion interactions in a uniform dispersion of precipitates. I_m is the mean value of saturation magnetisation for the two phase systems considered. There is some uncertainty in the values of K_1 and K_2, the magneto-crystalline anisotropy constants for nickel at and above room temperature; experimentally determined values of K_1 at 20° C vary between − 3.4 and − 5.8 × 10^4 ergs cm^{-3} [7, 8]. I_m in this case is calculated on a simple dilution basis from the saturation value $I_s = 484$ emu for pure nickel. The dashed lnes in fig. 5 represent equation 1 using the above two values of K_1 (this probably allows for any unknown contribution from K_2) and reasonable agreement is obtained with the experimental values. In the derivation of equation 1 only the reduction in magnetostatic energy involved in domain wall-precipitate interactions is allowed for and it is possible that the smaller calculated values of ΔH_c could arise from neglect of the reduction in domain wall energy in these interactions or some residual internal stress contribution (this point will be considered in section 3.3). At the same time it must be made clear that the dispersions of non-magnetic precipitates considered here are far from uniform (fig. 3a).

3.2. Coercivity and Precipitate Morphology

As stated previously, the coercivity of the oxidised alloys depended on the temperature of internal oxidation. Fig. 4 illustrates this dependence and shows a maximum coercivity over a small temperature range of oxidation for each of the three higher concentration alloys. The coercivity for the 0.058 wt % alloy showed a slight maximum for oxidation at about 1040° C. The size, shape and distribution of the internal oxide product has been fully discussed in [2] and [9].

The 0.48 wt % Si alloy shows the largest increase in coercivity at an oxidising temperature of about 1100° C. At this temperature the change

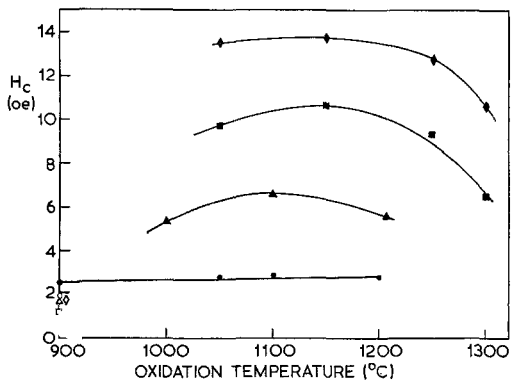

Figure 4 Room temperature measurements of the coercivity of the internally oxidised alloys as a function of the oxidising temperature.

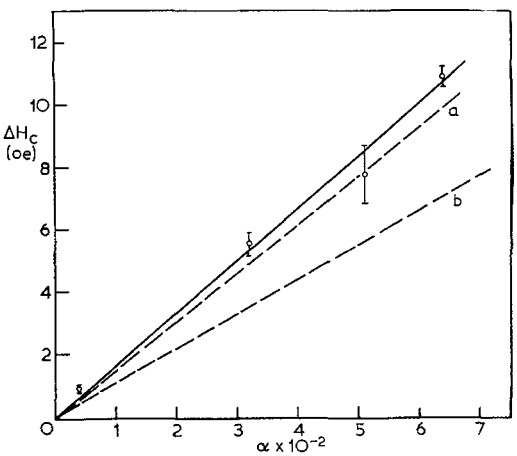

Figure 5 The increase in coercivity of the alloys due to internal oxidation as a function of volume fraction α of the oxide phase. Curves a and b are calculated values of $\triangle H_c(1)$ using $K = -5.8 \times 10^4$ and -3.4×10^4 ergs cm^{-3}.

of morphology of the precipitates with depth from the specimen surface, takes the form of a particulate zone to a depth of ~ 30 μm (particle size ~ 0.2 to 2.0 μm) and a mixture of filaments and networks of silica below this depth (e.g. fig. 3a). These filaments or fibres have orthogonal side-branchings (fig. 3b) and it is thought that these structures are responsible for the large increase in coercivity. Oxidation at 1000° C produces filamentary growths of a simpler form which are associated with a smaller coercivity. At ~ 1200° C the particulate zone extends to a greater depth and a smaller increase in coercivity results. The majority of particles precipitated are large enough to support subsidiary domain structures [10] and these structures may reduce the impeding effect on domain walls. The results obtained for this alloy show that coercivity is dependent to some extent on the morphology of the oxide product. This conclusion is supported by the results for the two more concentrated alloys which have the same form and a maximum in coercivity at oxidation temperatures between 1100 and 1200° C. In this temperature range side-branched filaments of silica are the most common product of oxidation. At lower temperatures where orthogonal growths are less prevalent the increase in coercivity is not so great. The effect of extended growths of silica on coercivity can definitely be inferred from oxidation at 1300° C when the particulate zone extends throughout the alloy section. There is a marked drop in coercivity associated with widely separated large spheroidal silica particles (~ 5 μm).

3.3. Temperature-Dependence of Coercivity

The dependence of coercivity on the temperature of measurement is of interest in the systems investigated because of the possibility of using these and like materials, i.e. oxide dispersion-strengthened ferromagnets [11, 12] in electrical machines in high temperature environments. For such an application the alloys should be magnetically "soft", hence the change in coercivity with temperature up to the Curie point of the matrix is of some importance.

The curves of fig. 6 show a linear decrease in coercivity of the alloys up to temperatures approaching the Curie point 360° C. This finding is in general agreement with the results of Towner *et al* [12] who investigated oxide (ThO_2) dispersion-strengthened Ni, Fe and Co. Also included in fig. 6 is a calculated curve for equation 1 and also curves for two equations due to Néel [6b] which give a stress contribution to coercivity, i.e. for $\lambda_s\sigma \gg K$

$$\Delta H_c(2) \simeq \beta \left(\frac{\lambda_s\sigma}{I_s}\right)\left[1.4 + \tfrac{1}{2}\ln\frac{6.8I_s^2}{1.5\lambda_s\sigma}\right] \quad (2)$$

and for $\lambda_s\sigma \ll K$

$$\Delta H_c(3) \simeq \frac{3\beta}{5\pi}\left(\frac{\lambda_s^2\sigma^2}{KI_s}\right)\left[1.4 + \tfrac{1}{2}\ln\frac{2\pi I_s^2}{K}\right] \quad (3)$$

The calculated curves apply to the 0.96 wt % Si alloy with the volume fraction of precipitate $\alpha = 0.64$. λ_s is the saturation magnetostriction constant of Ni, σ is an internal stress and β is the volume fraction of matrix subject to this stress It is clear that the calculated curve of ΔH_c (1)

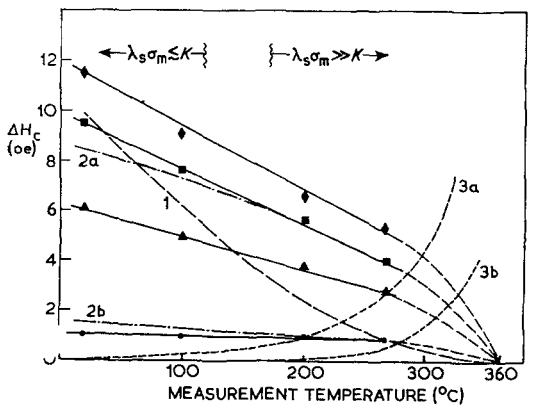

Figure 6 The increase in coercivity of the alloys due to internal oxidation as a function of the temperature of measurement of the hysteresis loop. Each specimen measured was that showing the maximum H_c at room temperature. Curve 1 is $\triangle H_c$ (1) for the 0.96 wt % Si alloy (♦), curves 2a and 2b are $\triangle H_c$ (2) for $\beta = 0.5\ \alpha$ and $0.1\ \alpha$ respectively, curves 3a and 3b are $\triangle H_c$ (3) for $\beta = 0.5\ \alpha$ and $0.1\ \alpha$ respectively.

due to inclusion impedance coercivity falls off more rapidly with temperature than the experimental curve. In the curves for the two possible stress-induced contributions, ΔH_c (2) and ΔH_c (3), β is assumed to be $0.5\ \alpha$ or $0.1\ \alpha$. There is no real reason for choosing these values for β except that any stress induced by the precipitate is not expected to be of very large range.

Two possible sources of stress in internally oxidised systems are (*a*) a shear stress in the isotropic metal lattice from a misfitting precipitate and (*b*) thermal stresses induced on cooling from the oxidising temperature, caused by differences in expansion coefficient of the matrix and precipitate. In the systems investigated here the silica precipitates are thought to be amorphous [13, 14], but crystalline trydimite has been reported in certain cases [4, 9, 15]. If amorphous the silica precipitates are certainly incoherent and if crystalline they are probably incoherent at the observed sizes of inclusion. In this situation, misfit strain E_M should be zero, but for coherent trydimite $E_M \simeq 0.1\delta \simeq 0.07$ (δ the conventional lattice misfit) [16] which leads to shear stresses of order 10^{11} dynes cm^{-2} and a condition $\lambda_S\sigma_M \gg K$ ($\lambda_S \simeq 3.4 \times 10^{-5}$ for Ni and $K = 5 \times 10^4$ ergs cm^{-3}) at least at high temperatures (fig. 6). In the case of thermal strains, $E_T \sim 5 \times 10^{-3}$ and hence $\sigma \sim 10^9$ dynes cm^{-2} and $\lambda_S\sigma_T \simeq K$ holds. Attempts to observe such matrix strains by diffraction contrast methods [17] have been unsuccessful and it could therefore be concluded that stress levels measurable by this technique are not present. As all the alloys reported on here were slow-cooled after internal oxidation, thermal strains should have been annealed out.

The calculated curves for ΔH_c (1) ΔH_c (2) in fig. 6 follow the downward trend of the experimental curves but agreement is not good. The curves for ΔH_c (2) have approximately the correct slope but fitting of these curves to experiment depends essentially on an arbitrary choice of β. The curves for equation 3 have entirely the wrong dependence and, of course, are not expected to

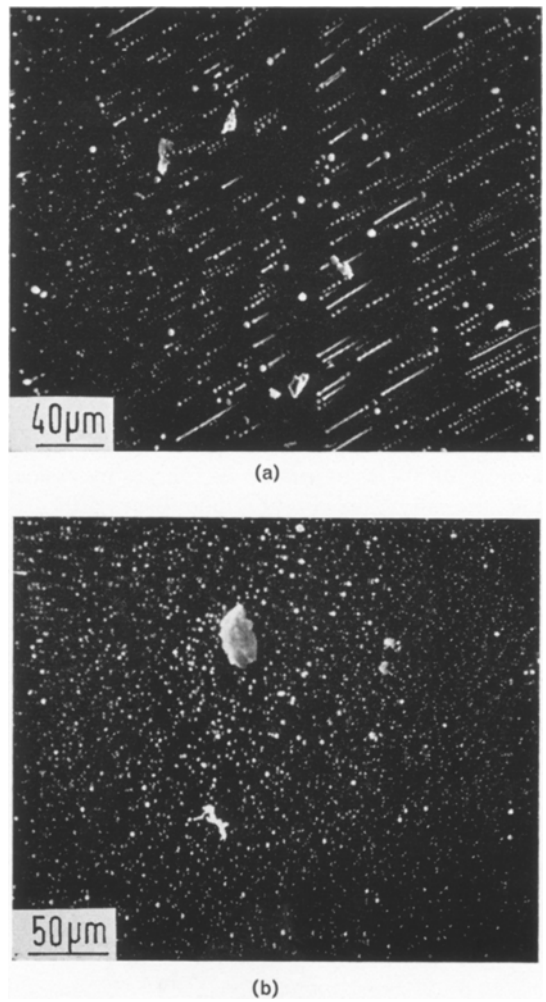

Figure 7 Scanning electron micrographs of sections of a Co-0.55 wt % Si alloy following extended heat-treatments after complete internal oxidation: (a) at 1250° C for 5 h showing spheroidisation of filaments of silica (× 225). (b) at 1165° C for 72 h showing possible precipitation ripening (× 200).

hold at high temperatures. The discrepancy between the curve for ΔH_c (1) and experiment is possibly due to a neglect of domain wall energy contributions and the choice of the temperature dependence of anisotropy and magnetostriction constants. However, as pointed out in section 3.1, the dispersions considered here are not particularly well suited to an application of the Néel equations in detail.

4. Conclusions

Results have been presented on the magnetic hysteresis properties of some internally oxidised Ni-Si alloys. Some attempts have been made to correlate the results, particularly coercivity, with the microstructure of the alloys. Unfortunately, because of the depth variation of precipitate morphology and precipitate size in the alloys, quantitative analysis of the results in terms of existent theories of coercivity is difficult. However, the general dependence of coercivity on precipitate morphology and volume fraction of precipitate has been established. Some explanation of the temperature dependence of coercivity to near the Curie point has been given. An exact analysis of this variation is not possible. Recent experiments on the stability of the extended growths and filaments of silica contained in these alloys and Co-Si alloys has shown that these forms can be degraded and spheroidised to give a more uniform dispersion of spheres by annealing the alloys at high temperature after the internal oxidation process, as illustrated in fig. 7. Similar results and conclusions on Cu-Si alloys have been obtained by Bolsaitis and Kahlweit [18]. Such dispersions would be more amenable to magnetic analysis and it is hoped to extend a structural and magnetic investigation to these systems.

Acknowledgements

Acknowledgements are due to the SRC for the award of a Research Studentship (R. B.) and to the Air Force Office of Scientific Research for support through the European Office of Aerospace Research, OAR United States Air Force under Grant EOOAR-68-005. Thanks are due to Professor R. S. Tebble for his continuing encouragement and support in this work.

References

1. R. BARLOW and P. J. GRUNDY, *J. Mater. Sci.* **4** (1969) 797.
2. R. BARLOW, P. J. GRUNDY, and B. JOHNSON, *ibid* **4** (1969) 359.
3. F. N. RHINES, *Trans. AIME* **137** (1940) 246.
4. S. GOTO, K. NOMAKI, and S. KODA, *J. Japan Inst. Met.* **31** (1967) 600.
5. P. VIGOUREUX and C. E. WEBB, "Principles of Electric and Magnetic Measurements" (Blackie and Sons Ltd, London 1947).
6. L. NÉEL, (*a*) *Ann. Univ. Grenoble* **22** (1946) 299; (*b*) *C.R. Acad. Sci. Paris* **223** (1946) 141 and 198.
7. G. AUBERT, *J. Appl. Phys.* **39** (1968) 504.
8. E. TATSUMOTO, T. OKAMOTO, N. IWATA, and Y. KADENA, *J. Phys. Soc. Japan* **20** (1965) 1541.
9. R. BARLOW, Thesis (1969) University of Salford.
10. J. B. GOODENOUGH, *Phys. Rev.* **95** (1954) 917.
11. A. C. BEILER, *J. Appl. Phys.* **38** (1967) 1161.
12. R. J. TOWNER, D. M. PAVLOVIC, and K. DETERT, *ibid* **39** (1968) 601.
13. S. L. CUNDY and P. J. GRUNDY, *Phil. Mag.* **14** (1966) 1233.
14. M. F. ASHBY and G. C. SMITH, *J. Inst. Metals* **91** (1962-63) 182.
15. P. J. NOLAN, private communication.
16. N. F. MOTT and F. R. N. NABARRO, *Proc. Phys. Soc.* **52** (1940) 86.
17. M. F. ASHBY and L. M. BROWN, *Phil. Mag.* **8** (1963) 1083 and 1649.
18. P. BOLSAITIS and M. KAHLWEIT, *Acta Met.* **15** (1967) 765.

Received 6 August and accepted 28 August 1970.